

# A SOFTWARE SYSTEM FOR EFFICIENT DEM SEGMENTATION AND DTM ESTIMATION IN COMPLEX URBAN AREAS

I. Van de Woestyne <sup>a</sup>, M. Jordan <sup>b</sup>, T. Moons <sup>a</sup>, M. Cord <sup>b</sup>

<sup>a</sup> Katholieke Universiteit Brussel, 1081 Brussels, Belgium, {*Ignace.VandeWoestyne*, *Theo.Moons*}@kubruessel.ac.be

<sup>b</sup> ETIS, UMR CNRS 8051, 95014 Cergy-Pontoise Cedex, France, {*cord*, *jordan*}@ensea.fr

**KEY WORDS:** DEM/DTM, segmentation, urban, semi-automation, three-dimensional, aerial, imagery, laser scanning.

## ABSTRACT:

Digital Elevation Models (DEMs) are a central information source for scene analysis, including specific tasks such as building localization and reconstruction. Whatever application is envisaged, DEM segmentation is a critical step, due to the great variability of landscapes and above-ground structures in urban areas. Moreover, a DEM may contain erroneous isolated 3D points which have to be identified before any interpretation process can start. Designing an automatic DEM segmentation method that is successful under all circumstances can hardly be envisaged. To facilitate the segmentation process, a user-friendly, interactive software environment, called ReconLab, has been developed. Its 3D viewing and editing capabilities allow to easily detect and remove erroneous 3D points from the initial data, to efficiently smooth the DEM and perform the segmentation in real time. ReconLab's usefulness for urban scene interpretation is demonstrated by applying it to the estimation of a Digital Terrain Model (DTM) from the DEM. In particular, ReconLab is used to perform a fast, semi-automatic segmentation of the DEM and to provide a significant and representative sample region consisting of ground points. These points are then used to initialize a parametric model for the terrain, which is iteratively refined by a robust algorithm. The preprocessing by ReconLab reduces computation time by a factor 3, without loss of accuracy, as is demonstrated by experiments on synthetic data and on real world DEMs obtained by airborne laser altimetry as well as by stereo correspondence from imagery.

## 1 INTRODUCTION

Many building reconstruction and scene interpretation systems use a Digital Elevation Model (DEM) — either generated from imagery by stereo or multiview correspondence or obtained from laser altimetry — as an essential information source. Whatever application is envisaged — e.g. orthophoto production, building reconstruction, (3D) road mapping, scene classification (such as building type, road type, vegetation type, etc.) — a critical step often is the segmentation of the DEM in regions of interest. Building reconstruction schemes usually use cadastre maps or manual procedures of some sort for building region delineation [see e.g. (Haala *et al.*, 1997, Jibrini *et al.*, 2000, Moons *et al.*, 1998, Roux & Maître, 1997, Vosselman & Suveg, 2001)]. Mapping and scene classification schemes, on the other hand, often rely on a ground–above ground separation of the DEM points [see e.g. (Baillard *et al.*, 1997, Collins *et al.*, 1995, Cord *et al.*, 2001, Paparoditis *et al.*, 2001)]. For dense urban areas complicating factors for this separation task are the relatively low number of ground points in comparison to above ground structures and — for a great number of towns in Europe — significant variations in terrain slope, in which case altitude is no longer an absolute indication for ground or above ground structures. Moreover, the identification of erroneous 3D data points in the DEM always remains an important point of attention.

In this paper a semi-automatic procedure is presented to efficiently extract a Digital Terrain Model (DTM) from a DEM of urban areas with significant variations in terrain slope and altitude. The line of reasoning consists of segmenting the DEM into connected surface regions, identifying the regions with the largest extent, verifying whether they belong to the ground level, and robustly fitting a parametric surface model to the ground points. Popular segmentation methods are based on watershed types of algorithm. Such an approach, however, may yield poor results when considerable variation in terrain slope and altitude

is present in the scene. The method presented in this paper maximally exploits the proximity of DEM points to perform the segmentation task, thus being less sensitive to surface slope or altitude. The segmentation algorithm is built into a user-friendly, multi-platform software system, called ReconLab. ReconLab was initially designed to be a 3D modeling and editing environment which allows easy and simultaneous visualization and manipulation of 3D data in connection with (one or more) images of the scene. The automatic altitude coloring and level curve capabilities of ReconLab on the 3D data as well as texture mapping from the images make it particularly easy to detect and remove erroneous segment parts from the regions of interest. In the final stage, a DTM is constructed by fitting a global parametric surface model to the ground segments using a robust estimation procedure which iteratively reduces the effect of (possibly remaining) above ground points on the surface parameters. It is demonstrated on real world data that the preceding segmentation of the DEM seriously improves the convergence speed of the fitting algorithm, without loss of accuracy on the resulting DTM. The different parts of the method and the experimental results are described in more detail in the subsequent sections.

## 2 IDENTIFYING CONNECTED SURFACE PARTS IN A DIGITAL ELEVATION MODEL

The first step in the construction of a DTM from a DEM is the identification of DEM points that belong to the ground level. To a large extent the ground surface in an urban scene is expected to be formed by DEM points corresponding to the road network and to open spaces such as parking lots, etc.. More formally, the terrain may be interpreted as a surface from which the buildings protrude. A DEM then is a sampling (as obtained from an airborne laser scanning e.g.) of the top surfaces of the urban scenery. Put differently, to some extent a DEM can be considered as being a discretization of a piecewise differentiable surface in 3-space.

Typically for the ground level (or road network) is that it corresponds to a connected differentiable surface part with low altitude (when compared to other DEM points) and which extends over the whole urban area represented in the DEM. Therefore, our segmentation algorithm aims at grouping DEM points that are expected to be samples from a connected differentiable surface patch. Moreover, since the algorithm must be able to cope with significant variations in slope and in altitude of the ground surface, “connectivity”, rather than “difference in altitude”, should be the crucial property for deciding whether neighbouring DEM points belong to the same connected surface component or not. This brings us to the following notions.

## 2.1 Definitions

Let  $r$  be positive real number. An  $r$ -path is a sequence of distinct DEM points  $(P_0, P_1, \dots, P_n)$  for which each  $P_i$  is contained in a sphere with radius  $r$  centered at  $P_{i-1}$  ( $i \in \{1, 2, \dots, n\}$ ). Two DEM points  $P$  and  $Q$  are said to be  $r$ -connectable, if there exists an  $r$ -path starting at  $P$  and ending at  $Q$ . Furthermore, a subset of a DEM is called  $r$ -connected, if any two DEM points in the subset are  $r$ -connectable. And, finally, an  $r$ -connected subset of a DEM is *maximally  $r$ -connected*, if it cannot be extended with additional DEM points and still remain  $r$ -connected.

## 2.2 Preprocessing

The aim of the segmentation algorithm is to extract the maximally  $r$ -connected subsets from a DEM. But some care has to be taken when using these notions in practice. Indeed, if DEM points are represented as triples  $(x, y, z)$  with  $(x, y)$  the coordinates of the scene point in some geographical reference system and with  $z$  being the altitude of that point in the scene, then, in an accurate DEM of an urban area, the difference in altitude between neighbouring DEM points will generally be much smaller than their distance in geographical location. Before applying the segmentation algorithm, the  $z$ -values of the DEM points are therefore multiplied with a positive constant  $\rho$ , in order to bring the modulus of these differences to the same order of magnitude as the generic distances in point location. Mathematically speaking, this means that a “sphere with radius  $r$  centered at  $P$ ” in the definitions above, in practice is an ellipsoid whose maximal horizontal section is a circle with radius  $r$  and whose smallest (vertical) axis is  $2r/\rho$ .

A second point of attention when dealing with real data is the presence of noise. Roughly speaking, the nastiest effect of noise in a DEM is that the altitude of a DEM point at a particular location deviates from its true value. If not taken into account, these arbitrary variations in altitude may cause an oversegmentation of the DEM: i.e. DEM points originating from one smooth connected surface patch may be split up in several small surface parts which are not semantically meaningful. This problem is commonly alleviated by smoothing the data before processing. If one assumes that structural errors have been removed from the DEM, then smoothing can be performed by a local averaging operation. But, as connectivity is the main segmentation criterion here, special care has to be taken that the borders of maximally  $r$ -connected regions are well preserved. Put differently, the altitude of DEM points lying at the borders of a maximally  $r$ -connected region may not be altered significantly by the smoothing process. Because  $r$ -connectivity boils down to be contained in a sphere with radius  $r$ , inverse distance weighting within such a sphere is adopted for smoothing. More precisely, for each DEM point  $P$ , all points  $P_i$  contained in a sphere with radius  $r$  centered at  $P$  are selected and their Euclidean distance  $d_i$  to  $P$  is computed. The smoothed  $z$ -value  $\tilde{z}$  for  $P$  now is the weighted

average

$$\tilde{z} = \frac{\sum_i w_i z_i}{\sum_i w_i} \quad \text{with} \quad w_i = \left(1 - \frac{d_i}{r}\right)^\alpha. \quad (1)$$

In practice,  $\alpha$  is usually set to 2. It is important to remark here that in our algorithm the smoothed altitude  $\tilde{z}$  does not replace the original, unscaled  $z$ -value of the DEM point  $P$ , but is added as a supplementary (fourth) coordinate. In this way, the original altitude measurements remain available at any time (e.g. to the DTM estimation algorithm to be applied later). Moreover, by the previous definitions, DEM points belonging to different segments (i.e. points belonging to different maximally  $r$ -connected regions) can never be  $r$ -connectable. Thus, even in the presence of noise, points belonging to one segment cannot significantly influence the  $z$ -values of points in another segment.

A third, and possibly the most important, point of attention when dealing with real data is the detection and removal of isolated points. Isolated points may result from errors in the measuring process (e.g. when using laser altimetry) or from errors in the disparity estimate (e.g. when the DEM is constructed by stereo correspondence from imagery), but they may also be due to correct measurements of points on building facades or originate from vegetation. Isolated points may result in tiny segments; or even worse, they may cause linkage of one surface patch to another, thus creating an  $r$ -path connecting two different surface patches and misleading the segmentation algorithm to create too large segments. Figure 1 illustrates these effects. In accordance with

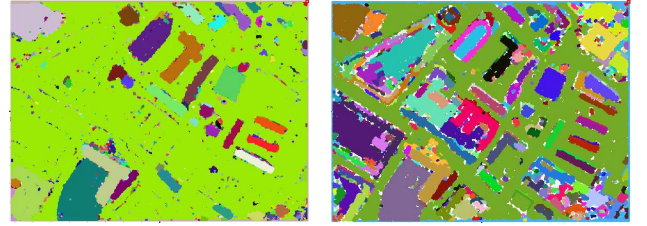


Figure 1: Left : Segmentation result without prior removal of isolated points (2219 regions). Right : Segmentation result with prior removal of isolated points (699 regions).

the previous definitions, an *isolated point* is a DEM point  $Q$  that counts less than a threshold number  $n$  of other DEM points in a sphere with radius  $r$  centered at  $Q$ . Isolated point removal can be performed iteratively: First, scan the DEM for isolated points (detection phase), then remove the detected isolated points (removal phase), and repeat the process until no more isolated points are found. Obviously, this procedure is very time consuming. But, as our first aim is to extract (sufficient) ground level points from the DEM to serve as input for the DTM surface estimation algorithm (in contradistinction to creating an accurate and semantically meaningful segmentation of the scene), there is no harm in occasionally removing some non-isolated points as well. In the experiments reported below, we therefore removed all points contained in a sphere with radius  $r$  centered at the isolated points detected in the first scan, and we did not iterate, in order to obtain the segmentation result in real time.

## 2.3 The segmentation algorithm

After the preparatory steps, the actual segmentation is performed. As mentioned before, a segment is defined here to be a maximally  $r$ -connected subset of the DEM. Segmentation thus can easily be performed iteratively by a region growing approach starting from an (arbitrary) DEM point that is not assigned to a segment

yet, and in which all points that are contained within a sphere of radius  $r$  centered at a segment point are assigned to that segment as well. But, the large number of data points in a dense DEM, on the one hand side, and the real time requirements we put forward for the segmentation algorithm, on the other hand, prompt us for another approach. Therefore, segmentation will be performed by an indexation procedure, which has the advantage that all DEM points have to be visited only once. The procedure comprises the following steps.

1. Start by indexing all the DEM points. If the DEM is constructed over a rectangular regular grid, then the  $(x, y)$ -coordinates of the DEM points can serve as the index. Moreover, if grid points would be missing in the DEM (e.g. due to occlusions in the imagery or because they were omitted during isolated point removal), then they may be given an (arbitrary negative)  $z$ -value which is a few multiples of  $r$  smaller than the minimal  $z$ -value of the DEM points. In this way, it will be possible to easily remove them later, while now maintaining the regularity of the grid. It is important to note, however, that, although a regular grid structure facilitates the indexing, it is not required for this algorithm.
2. Create a segmentation table. This is a dynamic table of lists of indices of DEM points that are  $r$ -connectable. Initially, the segmentation table is empty and will be updated in the subsequent steps.
3. Systematically scan the DEM and perform the following operations for every DEM point  $P$ .
  - (a) If the point at hand  $P$  does not belong to a previously constructed segment, then create a new segment number (index) in the segment table and assign this point to the new segment.
  - (b) Find all DEM points  $Q$  that are contained in a sphere with radius  $r$  centered at  $P$ .
  - (c) If some of these points  $Q$  already belong to a previously created segment, then all these segments, together with all the other points in the sphere around  $P$ , are merged by transferring the indexes of the involved DEM points to the entry corresponding to  $P$  in the segmentation table (cf. Figure 2). This is because all the DEM points in the segment of  $Q$  are  $r$ -connectable to  $P$ , and hence, by definition, belong to the same segment as  $P$ .
4. Update the segmentation table by removing segment indexes that contain no references to DEM points. This can easily be performed, because for each segment in the table, the number of DEM points in the reference list is stored as a separate entry.

| Segmentation table |     |            |
|--------------------|-----|------------|
| Index              | #   | References |
| 0                  | 4   | 2, 7, 8, 9 |
| 1                  | 3   | 1, 3, 4    |
| 2                  | 3   | 0, 5, 6    |
| ...                | ... | ...        |

| Segmentation table |     |                     |
|--------------------|-----|---------------------|
| Index              | #   | References          |
| 0                  | 0   |                     |
| 1                  | 7   | 1, 3, 4, 2, 7, 8, 9 |
| 2                  | 3   | 0, 5, 6             |
| ...                | ... | ...                 |

Figure 2: The segment with index 0 in the segment table is merged with the segment indexed 1 by moving the indexes of the DEM points in segment 0 to the reference list of segment 1.

Observe that, as the number of points in every segment is explicitly available, the segments can be sorted accordingly and

the largest regions (ground level) can easily be identified and selected. Results obtained by the segmentation algorithm on state-of-the-art DEMs are presented and discussed in section 4.

### 3 DTM ESTIMATION

The DEM points that belong to the segment corresponding to the ground level serve as input data for the estimation of a surface model for the terrain. The DTM estimation is performed by the algorithm presented in (Belli *et al.*, 2001, Jordan *et al.*, 2002). This section provides a brief overview of this algorithm. For more details on the estimation method and a discussion of its performance on a full DEM (i.e. including buildings and above ground areas), the interested reader is referred to those papers.

A DTM is modeled as a parameterized surface  $z(x, y)$ , where  $z(x, y)$  denotes the altitude of the scene point at geographic position  $(x, y)$ . As the terrain is assumed to vary smoothly, the function  $z(x, y)$  can be decomposed into a linear combination of 2D harmonic functions:

$$\begin{aligned}
 z(x, y) = & a_{0,0} \\
 & + \sum_{k,l=0; k+l \neq 0}^N a_{k,l} \cos[2\pi(k\nu_x x + l\nu_y y)] \\
 & + \sum_{k,l=0; k+l \neq 0}^N b_{k,l} \sin[2\pi(k\nu_x x + l\nu_y y)]
 \end{aligned} \tag{2}$$

with fundamental frequencies  $\nu_x = 1/T_x$  and  $\nu_y = 1/T_y$  for a DTM of size  $T_x \times T_y$ . The order  $N$  of the model can be seen as a constraint on the terrain variability. In fact, the main philosophy behind the method is that, if a DEM is considered as a surface, then the variations in altitude ( $z$ -values) caused by buildings and other above ground structures would mainly add to the high frequencies of the decomposition, whereas the terrain shape would mainly be represented by the low frequency terms. Hence, the idea is to model the DTM by a function of the form (2) with a low value for  $N$ , and to consider the above ground points in the DEM as being “structural noise” (outliers) that is present in the data.

The  $2(N+1)^2 - 1$  parameters in equation (2) are estimated from the coordinates  $(x_i, y_i, z_i)$  ( $i \in \{1, 2, \dots, m\}$ ) of the DEM points contained in the ground level segment obtained from the segmentation phase. Substituting these coordinates into equation (2) leads to an overdetermined system of linear equations

$$\mathbf{z} = \mathbf{M} \boldsymbol{\Theta} \tag{3}$$

with  $\mathbf{z} = (z_1, z_2, \dots, z_m)^t$ ,

$$\mathbf{M} = \begin{pmatrix} 1 & C_{0,1}(1) & S_{0,1}(1) & \dots & C_{N,N}(1) & S_{N,N}(1) \\ 1 & C_{0,1}(2) & S_{0,1}(2) & \dots & C_{N,N}(2) & S_{N,N}(2) \\ \vdots & \vdots & \vdots & \ddots & \vdots & \vdots \\ 1 & C_{0,1}(m) & S_{0,1}(m) & \dots & C_{N,N}(m) & S_{N,N}(m) \end{pmatrix},$$

where  $C_{k,l}(i) = \cos[2\pi(k\nu_x x_i + l\nu_y y_i)]$ ,

$S_{k,l}(i) = \sin[2\pi(k\nu_x x_i + l\nu_y y_i)]$  and with

$\boldsymbol{\Theta} = (a_{0,0}; a_{0,1}; b_{0,1}; \dots; a_{N,N}; b_{N,N})^t$ . A statistically robust solution to system (3) is obtained by using M-estimator theory, in which the influence of outliers — in this case, above ground DEM points — is iteratively reduced by minimizing a function  $\rho$  of the errors  $\epsilon_{\boldsymbol{\Theta}}(i)$  along the  $z$ -axis between the model predictions  $\mathbf{M}\boldsymbol{\Theta}(i)$  and the data  $z_i$ . The optimal solution thus is:

$$\boldsymbol{\Theta}_{\rho} = \arg \min_{\boldsymbol{\Theta}} \sum_{i=1}^m \rho(\epsilon_{\boldsymbol{\Theta}}(i)) \tag{4}$$

For the function  $\rho$  traditionally Tukey's norm is used. But keeping in mind that ground points systematically yield negative errors  $\epsilon_{\Theta}(i)$ , we use the asymmetric adaptation of Tukey's norm given by:

$$\rho_c(\epsilon) = \begin{cases} 0 & \text{if } \epsilon \leq 0 \\ \frac{c^2}{6} \left( 1 - \left( 1 - \left( \frac{\epsilon}{c} \right)^2 \right)^3 \right) & \text{if } 0 < \epsilon \leq c \\ \frac{c^2}{6} & \text{otherwise} \end{cases} \quad (5)$$

( $c$  is a scale factor). The weight function  $w_c$  corresponding to this norm is:

$$w_c(\epsilon) = \begin{cases} 1 & \text{if } \epsilon \leq 0 \\ \left( 1 - \left( \frac{\epsilon}{c} \right)^2 \right)^2 & \text{if } 0 < \epsilon \leq c \\ 0 & \text{otherwise} \end{cases} \quad (6)$$

Minimization of the object function proceeds iteratively till convergence by the weighted least-squares solution of the (iterated) system (3) :

$$\hat{\Theta}^{(k)} = \left( M^t W_c^{(k)} M \right)^{-1} M^t W_c^{(k)} \mathbf{z} , \quad (7)$$

where  $k$  is the iteration step and  $W_c^{(k)} = \text{diag} ( w_c(\epsilon^{(k-1)}) )$  is the diagonal weight matrix.

The iteration process is started by computing an initial DTM by means of a least-squares solution of the system (3) based on a random sample of DEM points from the full DEM, or on the DEM points contained in the ground level segment as obtained from the segmentation phase. In the subsequent iteration steps, the value of  $c$  is progressively decreased in order to reject more and more above ground DEM points as being "outliers", the weight matrix  $W_c^{(k)}$  is updated according to the new value of  $c$  and a new model estimate  $\hat{\Theta}^{(k)}$  is computed. The minimal and the maximal values of  $c$  are user-defined, but they must be chosen in accordance with the amplitude of the DEM and the minimal height of the above ground structures in the scene.

#### 4 EXPERIMENTAL RESULTS

The segmentation and the DTM surface fitting algorithm have been tested on state-of-the-art DEMs obtained through correspondence matching as well as from laser altimetry of several complex urban areas in France with various landscape types ranging from relatively flat and with modest constant slope to regions with large variations in terrain slope and altitude. In particular, the following three sorts of data were used in the experiments reported here.

**Synthetic DEM :** A synthetic DEM of size  $1024 \times 1024$ , which is generated as follows: First, an analytic "terrain" is computed as a sum of harmonic functions. Then five "buildings" are added to the terrain. These are rectangular block shapes with different heights. Finally, Gaussian noise is added to this analytic scene.

**DEM computed by stereo correlation :** This DEM is computed with the algorithm of (Cord *et al.*, 2001) on a stereo pair of scanned aerial images from the Hoengg dataset (Dataset Hoengg, 2001). The original images and the DEM are of dimensions  $1664 \times 1512$  and with a ground resolution of about  $10 \text{ cm}$  per pixel. The terrain slope on this area is approximately  $10 \text{ m}$ .

**Airborne laser DEM :** The third dataset is an airborne laser DEM, kindly provided to us by the Institut Géographique National (France). The complete DEM covers a  $2 \text{ km} \times 2 \text{ km}$  area on the center of Amiens (France), where each pixel has a ground resolution of  $20 \text{ cm}$ . In the experiments reported here, we used two sub-areas presenting various terrain slopes: The first one has dimensions  $1212 \times 1640$  and the second one covers an area of size  $2048 \times 2048$  in the city center.

First, the segmentation algorithm was applied to the data in order to test whether large portions of the ground level could be extracted in a (semi-)automatic manner. It turned out that, regardless of the terrain, the same parameter settings (i.e. the choices for the radii of the spheres — systematically denoted by  $r$  in section 2, — the scale factor  $\rho$  for scaling the  $z$ -coordinates, and the threshold  $n$  for isolated point detection) could be used for all DEMs with similar dimensions. Due to page restrictions, we are only able to present here the results obtained from one of the above mentioned dataset. Readers who are interested in a detailed discussion of the results of segmentation and DTM estimation on the other datasets as well are referred to (Van de Woestyne *et al.*, 2004). It is important to note, however, that the results described by means of the particular example below transfer to the other datasets as well.

Figure 3(a) shows one of the images of the first sub-area of the Amiens region (France). The corresponding part of the DEM, which was obtained through airborne laser scanning, is depicted in Figure 3(b). The coloring in Figure 3(b) represents the altitude of the corresponding scene point (with red indicating the highest value and blue the lowest). Figure 3(c) illustrates the effect of smoothing and of isolated point removal on the DEM in Figure 3(b). The scale factor  $\rho$  applied to the  $z$ -coordinates was set to 10 and the radii of the spheres used for both smoothing and isolated point removal was also set to 10. The threshold  $n$  for an isolated point was set to 4. Observe that mostly DEM points corresponding to building facades and vegetation are removed. Figure 3(d) shows the segmentation of the DEM, which was automatically obtained by the algorithm described in section 2.3. Here 12 was used as value for the radius in the definition of  $r$ -connectivity. Remark that a larger value for the radius of the spheres is used in the segmentation phase than for the preprocessing steps. The reason is that the radius  $r$  used in the preprocessing stage expresses some sort of error tolerance that is applied to the estimated altitude of the DEM points, whereas the radius  $r$  in the segmentation stage, on the contrary, represents the minimal separation distance between different surface patches in the scene.

As mentioned at the beginning of section 2, the ground level in dense urban areas is expected to be largely made up of the road network; and thus is likely to correspond to one of the largest DEM segments, to have low altitude when compared to the other segments, and, most importantly, to extend over the whole urban area represented in the DEM. Selecting the segment containing the largest number of DEM points in Figure 3(d) results in the area depicted in Figure 3(e). When a relative altitude coloring is applied to the segment (i.e. the coloring does not indicate absolute height values, but the colors red and blue respectively correspond to the highest and the lowest point in the segment itself), then possible errors immediately catch the eye. Indeed, a closer look to Figure 3(e) shows a red colored spot approximately in the middle of the figure and near the lower edge, whereas all the other DEM points in the segment obtain a blueish color. This indicates that the altitude of the spot seriously deviates from the average altitude of the rest of the segment. So, probably this is an error. In the introduction it is mentioned that the segmentation algorithm is built into a user-friendly, multi-platform software environment, called ReconLab. ReconLab was initially designed to



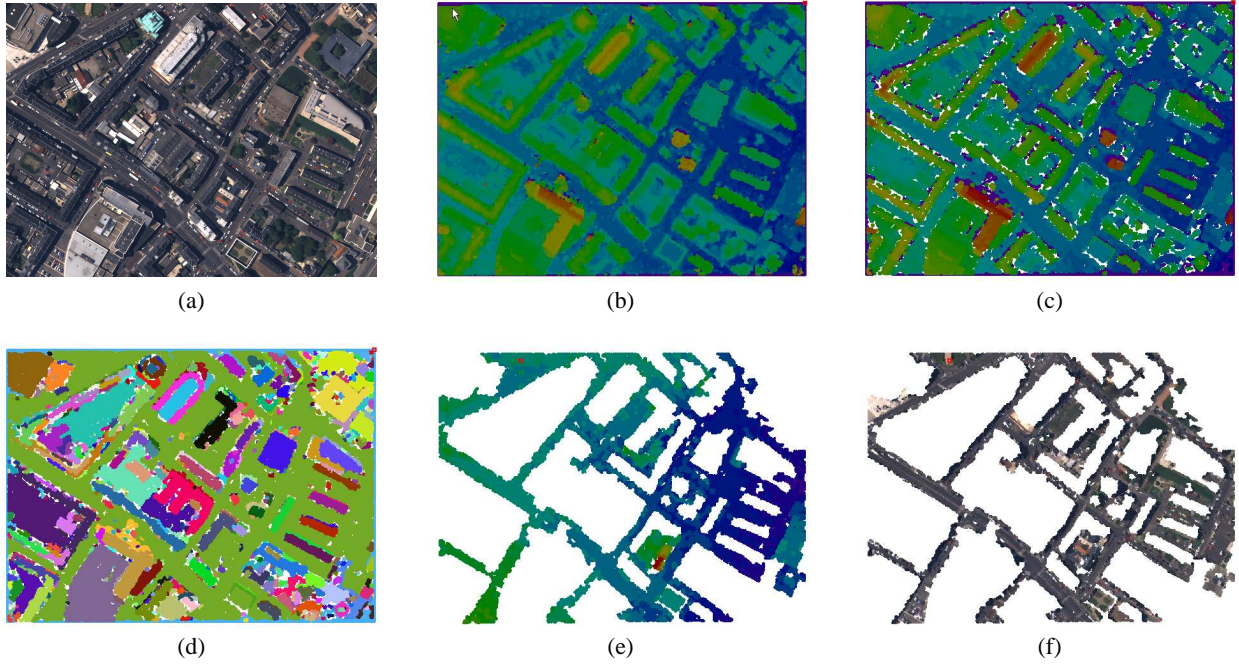


Figure 3: Results of ground level extraction for a sub-area of the airborne laser DEM of the Amiens region. (a) Part of an aerial image showing the sub-area of the Amiens region. (b) Part of the original DEM with altitude coloring. (c) The DEM part after smoothing and isolated point removal. (d) The result of automatic segmentation. (e) The automatically extracted ground level. (f) The extracted ground level with texture mapping for visual verification.

be a 3D modeling and editing environment which allows easy and simultaneous visualization and manipulation of 3D data in connection with (one or more) corresponding images of the scene, hereby automatically maintaining and updating structural relationships between the image features in the different views and with the 3D data. The different coloring modes used in these examples are basic features of ReconLab. But ReconLab also allows to map the image texture to the 3D information. Figure 3 (f) shows the same ground segment as in Figure 3 (e), but with the image texture mapped onto it. Zooming in to the red spot location proves that it indeed corresponds to a built up area, as expected. The editing capabilities of ReconLab allow to delineate and remove the erroneous area from the DEM segment with just a few mouse clicks. In this way, a fast and easy high-level user interaction between the automated components of the algorithm (i.e. segmentation and DTM surface fitting respectively) guarantees a qualitatively optimal surface model for the terrain. But even without this user interaction the DTM fitting algorithm does not suffer much from the possibly remaining errors in the selection of ground points, as is demonstrated next.

The segment corresponding to the ground level is used to initialize the DTM estimation algorithm described in section 3. Figure 4 shows the DTM surface model that was computed from the DEM points contained in the ground level segment of Figure 3 (f). For visualization purposes, *relative* altitude coloring was applied to the model. Therefore, the color pattern in Figure 4 is not the same as that in Figure 3 (e).

The usefulness of prior ground level extraction to DTM estimation has been tested on the other datasets as well. In particular, the algorithm was applied to each dataset twice: Once with the full DEM used for initialization, and once with starting from the DEM points contained in the ground level segment only. In the latter case, the initial DTM is a much better approximation of the real terrain, thus allowing to use a smaller maximum value of  $c$  and to have better and faster convergence of the algorithm. Apart from this, the algorithm was in each case applied with both

$N = 1$  and  $N = 2$  as the order of the DTM model. Execution times and number of iterations were recorded and compared for each test. Moreover, all tests are performed on an Intel Pentium IV processor running at 1.6 GHz, and a base 100 of normalized execution time was used for the  $N = 1$  DTM with initial data. The results are summarized in Table 1. Observe that convergence of the algorithm is improved by at least a factor 3 when initializing the DTM model with only the DEM points contained in the ground level segment provided by ReconLab, and without loss of accuracy. In fact, the difference between the DTM parameters  $\hat{\Theta}$  is less than 2% when obtained with or without initial segmentation. This also demonstrates the power of the DTM estimation algorithm in eliminating the above ground points during iteration when starting from the full DEM.

## 5 CONCLUSIONS

A user-friendly software system for semi-automatic real time filtering and segmentation of Digital Elevation Models is presented. The system is capable of extracting the ground level points from a dense DEM of complex urban areas, which show large variability in landscape and in terrain slope and altitude. The required user interactions are all high-level and mainly involve the supervision of the process. The quality of the extracted ground surface points is demonstrated by the fact that estimating a parametric DTM surface model from these points requires a computation time which is at least 3 times faster than without this preprocessing; and, there is no loss in accuracy of the resulting DTM. These observations were corroborated by test on a synthetically generated DEM and on real world DEMs obtained from airborne laser scanning as well as by stereo correspondence from imagery.

## REFERENCES

Baillard, C., Dissard, O., Jamet, O., and Maître, H., 1997. Extraction and characterization of above-ground areas in a peri-

| Synthetic dataset        |                          |                           |                           |
|--------------------------|--------------------------|---------------------------|---------------------------|
| with initial DTM         |                          | without initial DTM       |                           |
| $N = 1$<br>$c_{max} = 4$ | $N = 2$<br>$c_{max} = 4$ | $N = 1$<br>$c_{max} = 12$ | $N = 2$<br>$c_{max} = 12$ |
| 100<br>182 it.           | 1718<br>268 it.          | 213<br>393 it.            | 4794<br>753 it.           |

| Hoengg stereo correlation dataset |                          |                           |                           |
|-----------------------------------|--------------------------|---------------------------|---------------------------|
| with initial DTM                  |                          | without initial DTM       |                           |
| $N = 1$<br>$c_{max} = 4$          | $N = 2$<br>$c_{max} = 4$ | $N = 1$<br>$c_{max} = 20$ | $N = 2$<br>$c_{max} = 20$ |
| 100<br>54 it.                     | 1153<br>58 it.           | 238<br>128 it.            | 3217<br>135 it.           |

| Amiens airborne laser dataset |                          |                           |                           |
|-------------------------------|--------------------------|---------------------------|---------------------------|
| with initial DTM              |                          | without initial DTM       |                           |
| $N = 1$<br>$c_{max} = 5$      | $N = 2$<br>$c_{max} = 5$ | $N = 1$<br>$c_{max} = 20$ | $N = 2$<br>$c_{max} = 20$ |
| 100<br>23 it.                 | 1602<br>38 it.           | 322<br>91 it.             | 5774<br>139 it.           |

Table 1: Comparison of computation times and number of iterations for the DTM estimation initialized with or without ground level segmentation.

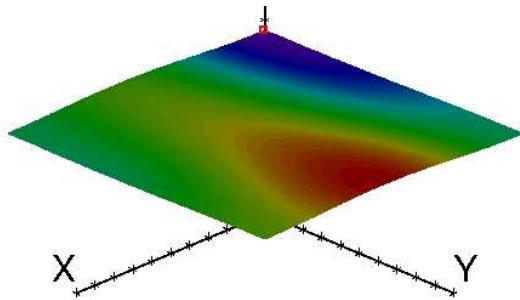


Figure 4: The DTM surface model with  $N = 2$  computed from the DEM points included in the ground level segment of Figure 3 (f). Relative coloring was applied for visualization.

urban context, in : Leberl, F., Kallian, R., and Grüber, M. (eds.), 1997. *Mapping Buildings, Roads and other Man-Made Structures from Images*, Schriftenreihe der Österreichischen Computer Gesellschaft, Band 92, R. Oldenbourg, Wien / München, pp. 159 – 174.

Baltsavias, E.P., Grün, A., and Van Gool, L., 2001. *Automatic Extraction of Man-Made Objects from Aerial and Space Images (III)*, Balkema Publishers, Lisse / Abingdon / Exton / Tokyo.

Belli, T., Cord, M., and Jordan, M., 2000. Colour contribution for stereo image matching, *Proc. International Conference on Colour in Graphics and Image Processing (CGIP'2000)*, Saint-Etienne, France, pp. 317 – 322.

Belli, T., Cord, M., and Jordan, M., 2001. 3D data reconstruction and modeling for urban scene analysis, in (Baltsavias *et al.*, 2001), pp. 125 – 134.

Collins, R.T., Hanson, A.R., Riseman M.R., and Schultz, H., 1995. Automatic extraction of buildings and terrain from aerial images, in (Grün *et al.*, 1995), pp. 169–178.

Cord, M., Jordan, M., and Cocquerez, J.-P., 2001. Accurate building structure recovery from high resolution aerial images, *Computer Vision and Image Understanding*, 82 (2), pp. 138 – 173.

Dataset Zürich Hoengg, 2001. Eidgenössische Technische Hochschule, Zürich, Switzerland, Project Amobe II. <http://www.igp.ethz.ch/p02/research/AMOBEdataset.html>.

Grün, A., Baltsavias, E.P., and Henricsson, O., 1997. *Automatic Extraction of Man-Made Objects from Aerial and Space Images (II)*, Birkhäuser-Verlag, Basel / Boston / Berlin.

Grün, A., Kübler, O., and P. Agouris, P., 1995. *Automatic Extraction of Man-Made Objects from Aerial and Space Images*, Birkhäuser-Verlag, Basel / Boston / Berlin.

Haala, N., Brenner, C., and Anders, K.-H., 1997. Generation of 3D city models from Digital Surface Models and 2D GIS, in : Baltsavias, E.P., Eckstein, W., Gülch, E., Hahn, M., Stallmann, D., Tempfli, K., and Welch, R. (eds.), 1997. *3D Reconstruction and Modelling of Topographic Objects*, International Archives of Photogrammetry and Remote Sensing, Vol. 32 Part 3-4W2, International Society of Photogrammetry and Remote Sensing, Sydney, pp. 68 – 76.

Jibrini, H., Paparoditis, N., Pierrot-Deseilligny, M., and H. Maître, H., 2000. Automatic building reconstruction from very high resolution digital stereopairs using cadastral ground plans, *Proc. 19th International ISPRS Congress*, Amsterdam, 2000.

Jordan, M., Cord, M., and Belli, T., 2002. Building detection from high resolution Digital Elevation Models in urban areas, in : Kallian, R., and Leberl, F., 2002. *ISPRS Commission III Symposium "Photogrammetric Computer Vision"*, Graz, Austria, IAPRS, XXXIV-3B, pp. 96 – 99.

Moons, T., Frère, D., Vandekerckhove, J., and Van Gool, L., 1998. Automatic modelling and 3D reconstruction of urban house roofs from high resolution aerial imagery, in : Burkhardt, H. and Neumann, B., 1998. *Computer Vision — ECCV'98*, LNCS 1406, Springer-Verlag, Berlin / Heidelberg / New York / Tokyo, pp. I.140 – I.425.

Paparoditis, N., Maillet, G., Taillandier, F., Jibrini, H., Jung, F., Guiges, L., and Boldo, D., 2001. Multi-image 3D feature and DSM extraction for change detection and building reconstruction, in (Baltsavias *et al.*, 2001), pp. 217 – 230.

Roux, M., and Maître, H., 1997. Three-dimensional description of dense urban areas using maps and aerial images, in (Grün *et al.*, 1997), pp. 311 – 322.

Van de Woestyne, I., Jordan, M., Moons, T., and Cord, M., 2004. DEM segmentation and DTM estimation in complex urban areas with ReconLab, Tournesol project T2003.05, Second annual report, 2004.

Vosselman, G., and Suveg, I., 2001. Map based building reconstruction from laser data and images, in (Baltsavias *et al.*, 2001), pp. 231 – 239.

## ACKNOWLEDGEMENTS

The authors gratefully acknowledge the support by the bilateral Belgian – French Tournesol exchange research grant, project no. T2003.05 “*Detection, reconstruction and visualization of 3D surface models from 3D point and line data*”, provided by the Ministry of the Flemish Community (Belgium) and the Ministry of Foreign Affairs (France). Special thanks and appreciation is also expressed to the Institut Géographique National (Saint-Mandé, France) for providing digital imagery and laser scan data used in the experiments.